AFRL-RX-WP-JA-2015-0101

ATOMISTIC SIMULATIONS OF SURFACE CROSS-SLIP NUCLEATION IN FACE-CENTERED CUBIC NICKEL AND COPPER (POSTPRINT)

D.M. Dimiduk, M.D. Uchic, and C. Woodward
AFRL/RXCM

S.I. Rao and T.A. Parthasarathy
UES, Inc.

APRIL 2014
Interim Report

STINFO COPY

AIR FORCE RESEARCH LABORATORY
MATERIALS AND MANUFACTURING DIRECTORATE
WRIGHT-PATTERSON AIR FORCE BASE OH 45433-7750
AIR FORCE MATERIEL COMMAND
UNITED STATES AIR FORCE

NOTICE AND SIGNATURE PAGE

//Signature//   //Signature//
_____   _____
MICHEAL E. BURBA, Project Engineer   DANIEL J. EVANS, Chief
Metals Branch   Metals Branch
Structural Materials Division   Structural Materials Division

//Signature//
_____
ROBERT T. MARSHALL, Deputy Chief
Structural Materials Division
Materials And Manufacturing Directorate

REPORT DOCUMENTATION PAGE

Form Approved
OMB No. 0704-0188

1. REPORT DATE *(DD-MM-YY)*	2. REPORT TYPE	3. DATES COVERED *(From - To)*
April 2014	Interim	19 March 2014 – 31 March 2014

4. TITLE AND SUBTITLE

ATOMISTIC SIMULATIONS OF SURFACE CROSS-SLIP NUCLEATION IN FACE-CENTERED CUBIC NICKEL AND COPPER (POSTPRINT)

5a. CONTRACT NUMBER
In-house

5b. GRANT NUMBER

5c. PROGRAM ELEMENT NUMBER
62102F

6. AUTHOR(S)

D.M. Dimiduk, M.D. Uchic, and C. Woodward - AFRL/RXCM

S.I. Rao and T.A. Parthasarathy - UES, Inc.

5d. PROJECT NUMBER
4349

5e. TASK NUMBER

5f. WORK UNIT NUMBER
X0W6

7. PERFORMING ORGANIZATION NAME(S) AND ADDRESS(ES)

AFRL/RXCM
2941 Hobson Way
Bldg 654, Rm 136
Wright-Patterson AFB, OH 45433

UES Inc.
4401 Dayton-Xenia Rd.
Dayton, OH 45432-1894

8. PERFORMING ORGANIZATION REPORT NUMBER

9. SPONSORING/MONITORING AGENCY NAME(S) AND ADDRESS(ES)

Air Force Research Laboratory
Materials and Manufacturing Directorate
Wright-Patterson Air Force Base, OH 45433-7750
Air Force Materiel Command
United States Air Force

10. SPONSORING/MONITORING AGENCY ACRONYM(S)
AFRL/RXCM

11. SPONSORING/MONITORING AGENCY REPORT NUMBER(S)
AFRL-RX-WP-JA-2015-0101

12. DISTRIBUTION/AVAILABILITY STATEMENT

Distribution Statement A. Approved for public release; distribution unlimited.

13. SUPPLEMENTARY NOTES

Journal article published in *Acta Materialia,* Volume 61, Issue 7 (2013) pp 2500-2508. ©2013 Elsevier Ltd. The U.S. Government is joint author of the work and has the right to use, modify, reproduce, release, perform, display or disclose the work. This report contains color. The final publication is available at http://dx.doi.org/10.1016/j.actamat.2013.01.026

14. ABSTRACT

In this manuscript, embedded atom potentials are used to determine the various core structures of glide screw-character dislocations intersecting free surfaces at right and inclined angles in face-centered cubic Ni and Cu. It is shown that the negative constriction forms at free surfaces under certain conditions. The role of various factors affecting the formation of negative constriction at the free surface, negative constriction energy, ledge annihilation and screw dislocation rotation due to Lothe's forces are discussed. The activation energy for surface cross-slip nucleation when the screw dislocation intersects the free surfaces at right angles, in the absence of ledge annihilation forces, is shown to be 0.05 eV in Ni and 0.09 eV in Cu. The activation-energy values obtained via the nudged elastic band method are significantly lower than the activation energy for cross-slip at attractive forest dislocation intersections in these materials. The present results are expected to be useful in understanding the mechanical behavior of micron-sized pillars under pure tension and compression.

15. SUBJECT TERMS

surface cross-slip, atomistic simulations, embedded atom potentials, nickel, copper

16. SECURITY CLASSIFICATION OF:			17. LIMITATION OF ABSTRACT:	18. NUMBER OF PAGES	19a. NAME OF RESPONSIBLE PERSON (Monitor)
a. REPORT	**b. ABSTRACT**	**c. THIS PAGE**	SAR	12	Micheal E. Burba
Unclassified	Unclassified	Unclassified			**19b. TELEPHONE NUMBER** *(Include Area Code)* (937) 255-9795

Atomistic simulations of surface cross-slip nucleation in face-centered cubic nickel and copper

S.I. Rao [a,*], D.M. Dimiduk [b], T.A. Parthasarathy [a], M.D. Uchic [b], C. Woodward [b]

[a] *UES, Inc., 4401 Dayton-Xenia Rd., Dayton, OH 45432-1894, USA*
[b] *Air Force Research Laboratory, Materials and Manufacturing Directorate, AFRL/MLLM Wright-Patterson AFB, OH 45433-7817, USA*

Abstract

In this manuscript, embedded atom potentials are used to determine the various core structures of glide screw-character dislocations intersecting free surfaces at right and inclined angles in face-centered cubic Ni and Cu. It is shown that the negative constriction forms at free surfaces under certain conditions. The role of various factors affecting the formation of negative constriction at the free surface, negative constriction energy, ledge annihilation and screw dislocation rotation due to Lothe's forces are discussed. The activation energy for surface cross-slip nucleation when the screw dislocation intersects the free surfaces at right angles, in the absence of ledge annihilation forces, is shown to be 0.05 eV in Ni and 0.09 eV in Cu. The activation-energy values obtained via the nudged elastic band method are significantly lower than the activation energy for cross-slip at attractive forest dislocation intersections in these materials. The present results are expected to be useful in understanding the mechanical behavior of micron-sized pillars under pure tension and compression.
© 2013 Acta Materialia Inc. Published by Elsevier Ltd. All rights reserved.

Keywords: Surface cross-slip; Atomistic simulations; Embedded atom potentials; Nickel; Copper

1. Introduction

There is increasing recognition of the need to incorporate physics-based models of deformation in the design of structural components. While models for predicting yield strength and creep behavior are beginning to incorporate significant physics, models for fatigue, ultimate strength and ductility remain mostly empirical. This is because strain-hardening and fatigue resistance are strongly influenced by dislocation micromechanisms, especially cross-slip, and including physics-based cross-slip processes in mesoscale simulations has been difficult. The early work of Escaig remains the most widely cited and used model for cross-slip wherein the screw dislocation locally constricts and immediately redissociates on the cross-slip plane [1]; however, this model poses several difficulties with respect to quantitative simulations. The model is highly sensitive to choice of parameters that have thus far been difficult to quantify. For example, the constriction width required for cross-slip is unknown but significantly influences the energetics of the cross-slip process [2]. This difficulty has led to an ad hoc postulate that obstacles always exist in materials and that they enable sufficient dislocation core constriction under normal stresses, thereby ensuring cross-slip [3]. Aside from being unsatisfactory, this forces cross-slip models (particularly for single crystals) to make arbitrary assumptions about dislocation obstacle spacings. Advances in atomistic simulations offer the possibility of gaining insights into the cross-slip process that may serve to enable mesoscale simulations to accurately capture the atomic-level physics of a dislocation process.

Atomistic simulation studies from the late 1990s were limited to calculating constriction energies and energetics of cross-slip using a single dislocation in a periodic unit cell [2,4]. These simulations helped to unravel some interesting and useful aspects of cross-slip which were unanticipated.

* Corresponding author. Tel.: +1 9372551318; fax: +1 9372553007.
  E-mail addresses: satish.rao@wpafb.af.mil, satish.rao.ctr@wpafb.af.mil (S.I. Rao).

The most important finding was that configurations exist for which one of the pair of constrictions has a negative energy [2,4]. Thus spontaneous nucleation of cross-slip is possible so long as only one constriction is needed, as is the case for surface nucleation. However, previous atomistic simulations [4] of a screw-character dislocation intersecting free surfaces at right angles in face-centered cubic (fcc) Cu have shown that the screw dislocation prefers to reside on a {1 1 1}-type plane parallel to the surface ledge on which it was created, without easy cross-slip nucleation. This is in contrast to recent atomistic simulation results of screw-character dislocations intersecting mildly attractive and repulsive forest dislocations in the bulk in fcc Ni, where cross-slip has been shown to occur easily [5–8]. In this work, the possibility of cross-slip at dislocation–surface intersections in fcc Ni and Cu was examined using large-scale atomistic simulations. A glide screw dislocation that intersects two free surfaces perpendicularly as well as in an inclined fashion is modeled and it is shown that several conditions exist where surface cross-slip can nucleate easily. This, we believe, has the potential to explain dislocation multiplication in low-density micron-sized fcc pillars subjected to a uniform tensile or compressive loading.

We have performed molecular statics simulations of screw dislocation intersections with free surfaces for the [1 1 1] and [1 0 0] orientations, with the screw dislocation having a Burgers vector of 1/2 [1 $\bar{1}$ 0]. Section 2 describes the simulation technique and the interatomic potentials used for the simulations, Section 3 presents the core structures obtained from atomistic simulations. Section 4 describes activation energy calculations for surface cross-slip when the screw dislocation intersects the free surfaces at right angles, in the absence of ledge annihilation forces. Finally, Sections 5 and 6 give a discussion and summary of the results, respectively.

2. Simulation technique

The atomistic simulations described here employed the three-dimensional (3-D) parallel molecular dynamics code, LAMMPS [9], developed at Sandia National Laboratory. The simulation cell is a rectangular parallelepiped, with the z-axis oriented along the [1 1 1] or [1 0 0] directions. For the z-axis oriented along [1 1 1], the dimensions of the simulation cell along the z-axis was ∼15 nm, the dimension along the x-axis was ∼30.0 nm and along the y-axis ∼15 nm. For the z-axis oriented along [1 0 0], the dimensions of the simulation cell along the z-axis was ∼40 nm, the dimension along the x-axis was ∼14 nm and along the y axis ∼14 nm. This corresponds to approximately 1 million atoms in the simulation cell. A 1/2 [1 $\bar{1}$ 0] screw dislocation is inserted in the middle of the simulation cell using its anisotropic elastic displacement field [10]. Unless otherwise specified, the plane of the cut performed to generate the screw dislocation was the (1 1 1) glide plane. In the activation energy calculations, the cube plane cut was used. The origin for the initial anisotropic displacement field of

the screw dislocation was varied to obtain several different core structures for the screw dislocation interaction with the free surfaces. Fixed boundary conditions were applied along the z and y directions and energy minimization was performed using the conjugate gradient technique. Free surface boundary conditions were applied along the x direction.

2.1. Interatomic potential

The embedded atom potential used in the simulations is the potential developed for fcc Ni by Angelo, Moody and Baskes [11] (hereafter termed the Moody potential) based on the Voter and Chen format as well as the embedded atom potential developed for fcc Ni by Mishin [12]. For fcc Cu, an embedded atom potential developed by Mishin et al. is used [13]. Table 1 gives the lattice parameter, cohesive energy, elastic constants and stacking fault energy given by the Mishin and Moody potentials for fcc Ni as well as the Mishin potential for fcc Cu.

2.2. Depiction of core structures

In some figures, to depict core structures we use the method developed by Stukowski and Albe [14] which extracts dislocation lines and their associated Burgers vectors from 3-D atomistic simulations. It is based on a fully automated Burgers circuit analysis, which locates dislocation cores and determines their Burgers vector. The transition from the atomistic system to a discrete dislocation representation is achieved through a subsequent vectorization step.

In order to illustrate the relaxed screw dislocation geometries, in some figures, we take advantage of the increase in atomic energy produced by the strain field of the partial dislocations. By plotting the atoms with assigned energies within LAMMPs of greater than −4.42 eV (Ni) or 3.52 eV (Cu) (the energy of atoms in the stacking fault region), the partial dislocations can be imaged easily even in these large simulation cells [5–7]. In order to illustrate the cross-slipped-segment products of the screw dislocation, the positions are shown in a [1 1 $\bar{2}$] projection as well as the [1 1 1] projection. In the [1 1 $\bar{2}$] projection segments spread on the initial (1 1 1) plane appear as a single line and cross-slipped segments (i.e. on a (1 1 $\bar{1}$) plane) appear

Table 1
Lattice parameter, a_0, cohesive energy, E_c, elastic constants, C_{11}, C_{12} and C_{44}, and stacking fault energy, γ, given by the Moody embedded atom potential for Ni, and the Mishin embedded atom potentials for Ni and Cu.

Property	Ni (Mishin)	Ni (Moody)	Cu (Mishin)
a_0 (A)	3.52	3.52	3.615
E_c (eV)	−4.45	−4.45	−3.54
C_{11} (×10^{11} N m^{-2})	2.41	2.46	1.70
C_{12} (×10^{11} N m^{-2})	1.51	1.47	1.23
C_{44} (×10^{11} N m^{-2})	1.27	1.25	0.76
γ (mJ m^{-2})	134	89	44

as a pair of partials separated by a stacking fault. This method of depicting the core of the screw dislocation also readily shows the sense of rotation of the screw dislocation at the free surfaces.

3. Screw dislocation intersecting the free surfaces at right angles

Figs. 1 and 2 give a dislocation line representation of the core structure obtained for the screw dislocation–surface interaction when the screw dislocation intersects the free surfaces at right angles using the Mishin potential for Ni. The z-axis is along [1 1 1], the x- and y-axes are along [1 $\bar{1}$ 0] and [1 1 $\bar{2}$], respectively. In Figs. 1 and 2, a 1/2 [1 $\bar{1}$ 0] screw dislocation, passing approximately through the origin, was initially inserted into the simulation cell using its anisotropic elasticity displacement field, with several slightly different elastic centers for the displacement field. The cut for the initial elastic displacement field was made on the [1 1 1] glide plane. Depending upon the elastic center position, either the core structure shown in Fig. 1 or that shown in Fig. 2 was obtained, having the screw dislocation either fully residing on the (1 1 1) glide plane (Fig. 1) or residing partially on the (1 1 1) glide plane and partially on the (1 1 $\bar{1}$) cross-slip plane (Fig. 2). The core structure with the screw dislocation completely on the (1 1 $\bar{1}$) cross-slip plane never materialized. Similar results were obtained with the Moody potential for Ni as well as the Mishin potential for Cu. In Fig. 1, the screw dislocation is constricted at the positive 'x' surface, whereas it is expanded at the negative 'x' surface. This is due to the effect of Escaig stress components acting on the Shockley partials arising from image stresses at the free surfaces and has been predicted using continuum elasticity theory [15–17]. In addition, in Fig. 2, the screw dislocation is bent inwards (toward the positive 'y' direction) at both free surfaces. This, we believe, results in an annihilation of ledge surface area at the free surfaces since the screw dislocation was formed by performing a (1 1 1) plane cut. The ledge annihi-

lation forces are balanced by line tension forces at equilibrium and this is the reason why the screw dislocation prefers to reside on the plane on which the initial cut was performed. To interrogate the screw dislocation behavior at free surfaces without the ledge annihilation effect, several simulations having slightly different initial elastic centers were performed, with the screw dislocation formed using a (0 0 1) cube plane cut instead of a (1 1 1) plane cut, again using the Mishin potential for Ni. In this case, four different core structures were obtained for the screw dislocation as shown in Fig. 3a–d in a 3-D dislocation line representation. For two of the four different core structures, the screw dislocation is partially cross-slipped via the spontaneous formation of a negative constriction [2] and the two core structures are equivalent by symmetry. The other two core structures, one residing fully on the glide plane and one fully residing on the cross-slip plane, are also crystallographically equivalent to each other. Similar results were obtained with the Moody potential for Ni as well as with the Mishin potential for Cu. In these simulations, the dissociation of the screw dislocation either on the (1 1 1) glide plane or on the (1 1 $\bar{1}$) cross-slip plane results in extra ledge surface area formation at the free surfaces. However, the fully glide plane as well as the fully cross-slip plane core structures are completely constricted at one of the free surfaces (from Escaig stresses induced by image stresses), whereas the partially cross-slipped core structures are spread out at both free surfaces. Therefore, the energy of the partially cross-slipped core structures relative to the fully glide plane or fully cross-slip plane core structures, $\delta\gamma$, can be approximately written as $\partial\gamma = 0.5(\gamma_l db + E_n)$, where E_n is the formation energy of a negative constriction [2], b is the Burgers vector of the screw dislocation, d is the Shockley partial spacing of the partially cross-slipped core structure at the free surface and γ_l is the free surface ledge energy per unit area. Taking $d \approx 4 - 5b$ [7], and the negative constriction formation energy as ~ -1.23 eV [7] for the Mishin potential for Ni, and with $\delta\gamma$ determined as -0.06 eV from the simulations, one obtains the free surface
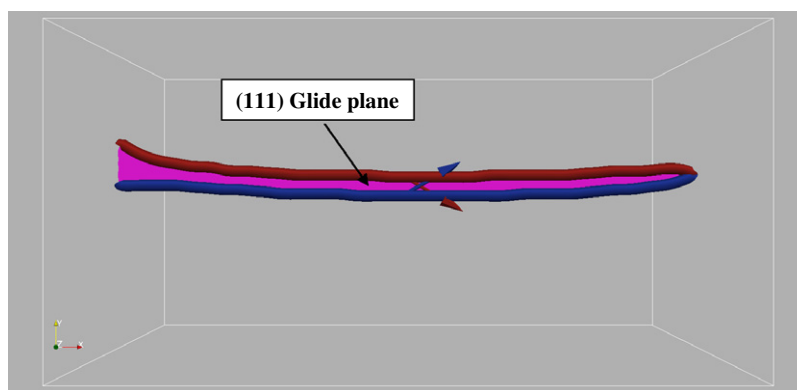

Fig. 1. A 3-D dislocation line representation of the fully glide plane structure formed for a ½[1 $\bar{1}$ 0] screw dislocation intersecting two free surfaces at right angles. The screw dislocation was formed with a (1 1 1) glide plane cut. The x-axis is along [1–10], the y-axis is along [1 1 $\bar{2}$] and the z-axis is along [1 1 1]. The stacking fault region is shaded in pink. The colored arrows denote the Burger's vector magnitude and direction of the Shockley partials. (For interpretation of the references to colour in this figure legend, the reader is referred to the web version of this article.)
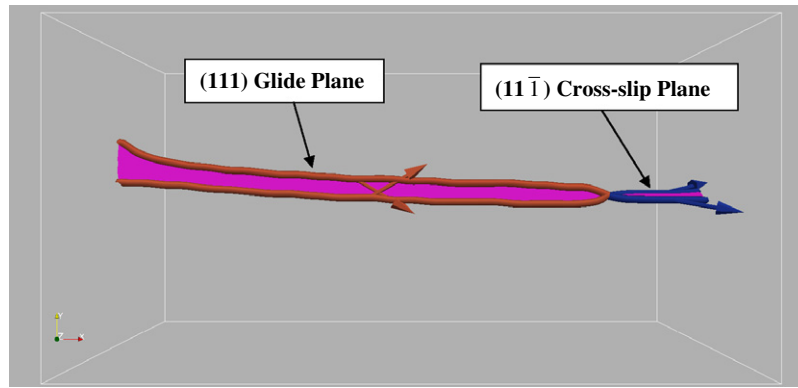
3

Fig. 2. A 3-D dislocation line representation of the partially cross-slipped structure formed for a ½[1 $\bar{1}$ 0] screw dislocation intersecting two free surfaces at right angles. The screw dislocation was formed with a (111) glide plane cut. The x-axis is along [1 $\bar{1}$ 0], y axis is along [11 $\bar{2}$] and the z-axis is along [1 1 1]. The stacking fault region is shaded in pink. The colored arrows denote the Burger's vector magnitude and direction of the Shockley partials. (For interpretation of the references to colour in this figure legend, the reader is referred to the web version of this article.)

ledge energy γ_1 as 550–675 mJ m^{-2}. This value is approximately one-third the (111) surface energy given by the Mishin potential for Ni [12]. Using the Mishin potential for Cu, $E_n \approx -1.3$ eV, $\delta\gamma \approx 0.01$ eV, $d \approx 6b$ [6,7] gives the free surface ledge energy γ_1 as 538 mJ m^{-2}, which as before is approximately one-third the (111) surface energy given by the Mishin potential for Cu [13]. With the Moody potential for Ni, $E_n \approx -1.58$ eV, $\delta\gamma \approx 0.14$ eV, $d \approx 6b$ [5–7] gives the free surface ledge energy γ_1 as 555 mJ m^{-2}, which is also approximately one-third the (111) surface energy given by Ni Moody potential for Ni [11]. We will discuss below the application of the nudged elastic band (NEB) method [7,18] with the initial and final states as the fully glide plane and partially cross-slipped structures of Fig. 3a–d to obtain the activation energy for surface cross-slip nucleation in fcc Ni in the absence of ledge annihilation forces.

3.1. Screw dislocation intersecting the free surfaces in an inclined fashion

In the simulation results to be described in this section the screw dislocation was initially inserted in the simulation cell using its anisotropic elasticity displacement field with a (111) glide plane cut. For the z-axis oriented along one of the multi-slip or single slip orientations, [100] or [011] or [1 $\bar{1}$ 1] or [4 $\bar{1}$ 3], the screw dislocation intersects the free surfaces in an inclined fashion. Figs. 4 and 5 depict two different core structures obtained for the screw dislocation intersecting (010) free surfaces at 45° using the Mishin potential for Ni both in the [111] and [11 −2] projections as well as the 3-D dislocation line representation. The simulation cell used to obtain the core structures shown in Figs. 4 and 5 had the z-axis oriented along [100], the x-axis along [010] and the y-axis along [001] with fixed boundary conditions along "y" and "z" and free surface boundary conditions along "x". Figs. 4 and 5 clearly show the rotation of the screw dislocation to minimize its energy due to Lothe's forces [15–17]. The screw dislocation, as it

rotates, decreases its line length, whereas its line energy per unit length increases since it moves away from the screw orientation. This results in an equilibrium line orientation for the screw dislocation where its total line energy is a minimum. Note that for this orientation of the simulation cell, the expected rotations on both the (111) glide plane and the (11 $\bar{1}$) cross-slip plane are identical at equilibrium. For one core structure, the screw dislocation completely resides on the (111) glide plane whereas for the other core structure, the screw dislocation is partially cross-slipped onto the (11 $\bar{1}$) cross-slip plane with the formation of a negative constriction. For both core structures, there is ledge annihilation at the negative "x" surface and ledge formation at the positive "x" surface due to the rotation. The energy of the partially cross-slipped core structure is lower relative to that of the fully glide plane core structure by ~1 eV. If the Burgers vector of the screw dislocation is reversed, then the formation of a partially cross-slipped core structure requires the screw dislocation to be on the cross-slip plane on the negative "x" side and on the glide plane on the positive "x" side, which requires extra ledge formation on both surfaces and is energetically prohibitive. Therefore, depending upon the sense of rotation, it is energetically favorable to form the partially cross-slipped core structure for only one sense of the screw dislocation Burger's vector, either positive or negative. Similarly, the fully glide plane as well as the partially cross-slipped core structures having a negative constriction were observed for simulation cells with the z-axis oriented along [4 $\bar{1}$ 3], [011] and [1 $\bar{1}$ 1]. In these simulations, the free "x" surfaces were chosen such that the amount of rotation of the screw dislocation due to Lothe's forces were identical on the (111) glide plane and the (11 $\bar{1}$) cross-slip plane. In all cases, the partially cross-slipped core structure formed for only one sense of the screw dislocation Burgers vector and had a lower energy as compared to the fully glide plane core structure. The fact that there is a local minimum in energy at both the fully glide plane state as well as the partially cross-slipped state suggests that there is a finite activation barrier for
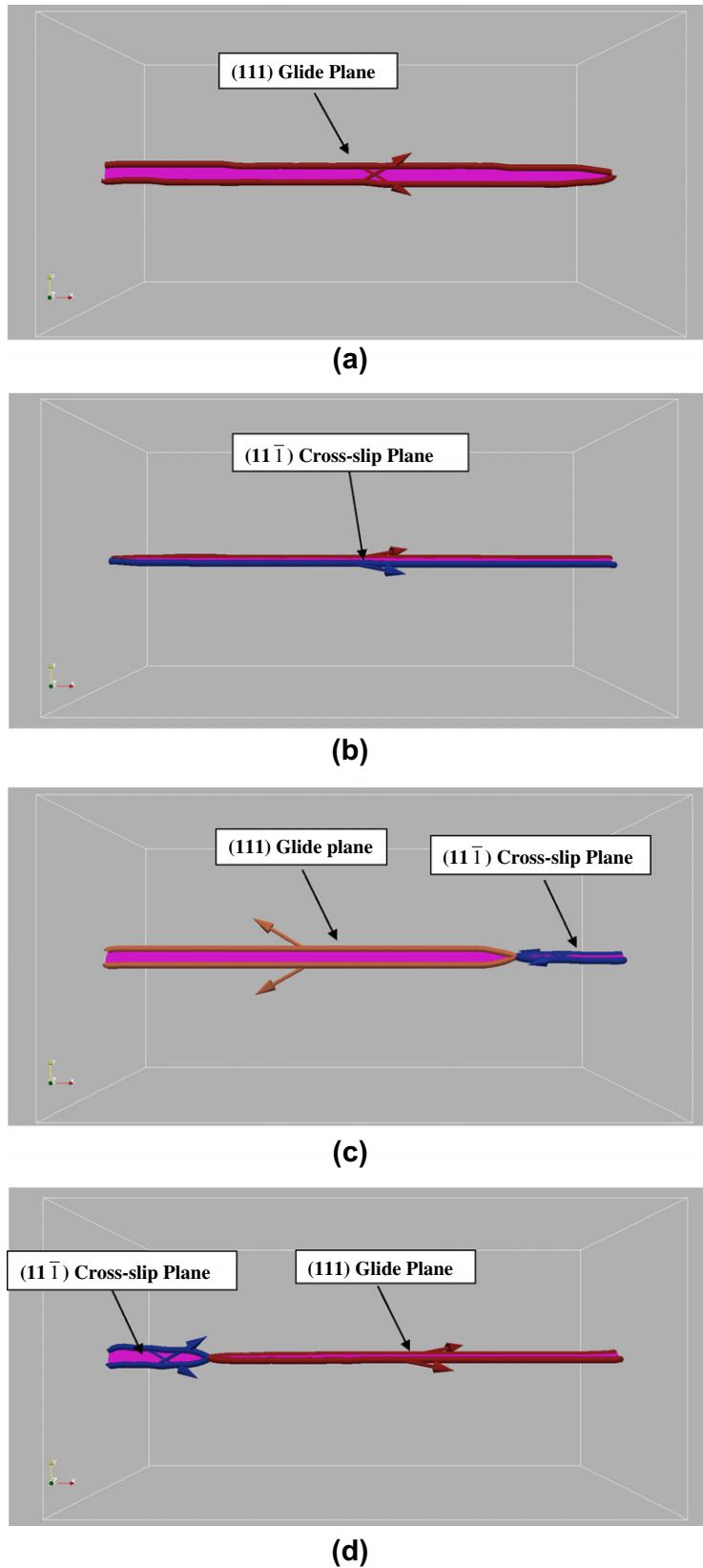
Fig. 3. A 3-D dislocation line representation of the fully glide plane structure (a), fully cross-slip plane structure (b), partially cross-slipped structures 1 and 2 (c and d) formed for a ½[1$\bar{1}$0] screw dislocation intersecting two free surfaces at right angles. The screw dislocation was formed with a (001) cube plane cut. The *x*-axis is along [1$\bar{1}$0], the *y*-axis is along [11$\bar{2}$] and the *z*-axis is along [111]. The stacking fault region is shaded in pink. The colored arrows denote the Burger's vector magnitude and direction of the Shockley partials. (For interpretation of the references to colour in this figure legend, the reader is referred to the web version of this article.)

5

surface cross-slip [7], though it is expected to be small as shown later. However, the amount of ledge annihilation and screw dislocation rotation may not be identical between the fully glide plane and the partially cross-slipped structures, and therefore the determination of activation energy for surface cross-slip nucleation becomes problematic for this geometry.

4. Surface cross-slip nucleation activation energy in the absence of ledge annihilation forces

The NEB method [7,18] was used to determine the activation energy for surface cross-slip nucleation in the absence of ledge annihilation forces. The fully glide plane state and the partially cross-slipped state of Fig. 3a–d were taken as the initial and final states for the NEB calculations. A total of 16 replicas (including the initial and final states) were used in the NEB calculations, together with an inter-replica spring constant of 0.04 eV A^{-2} [7]. Constrained energy minimization for these calculations were performed using a damped dynamics technique for up to

20,000 fs [5]. The NEB calculations were used to determine the energy profile as the screw dislocation transformed from the fully glide plane state to the partially cross-slipped state. The energy profile shows a maxima in between the initial and final states corresponding to the activated state. The energy difference between the activated state and the fully glide plane state (initial state) was taken to be the activation energy for surface cross-slip nucleation in the absence of ledge annihilation forces. Fig. 6 shows the [1 1 1] and [1 1 $\bar{2}$] projections of the activated state obtained using the Ni Mishin potential. The activated state has a very small portion of the screw dislocation on the cross-slip plane. The activation volume for surface cross-slip nucleation with respect to Escaig stresses can be estimated from the area of this small cross-slipped portion to be extremely small. The activation energy for surface cross-slip nucleation was found to be ~0.05 eV with the Mishin potential for Ni. Similar NEB calculations were performed with the Moody potential for Ni as well as the Mishin potential for Cu and the activation energy for surface cross-slip nucleation was determined to be ~0.20 and ~0.09 eV, respec-
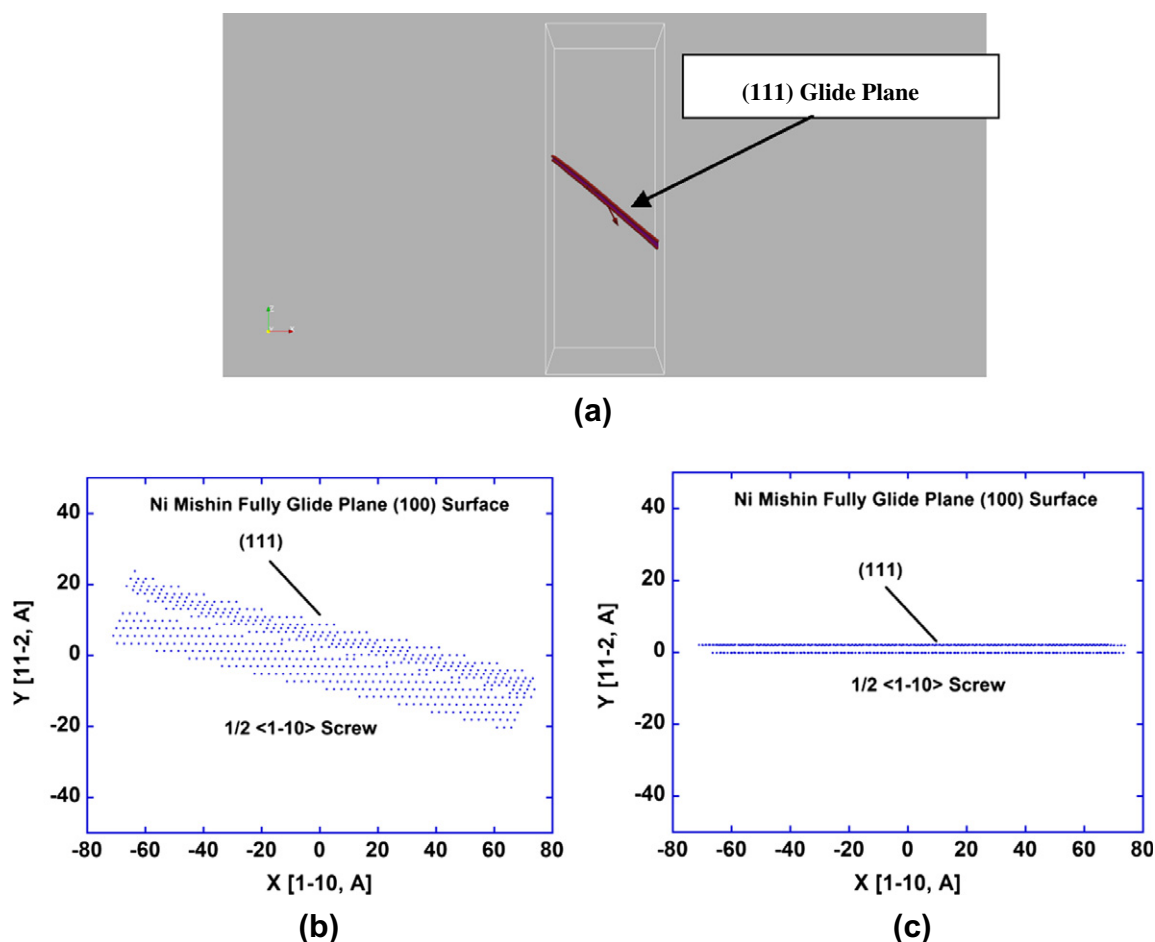

(a)

(b)

(c)

Fig. 4. A 3-D dislocation line representation (a) of the fully glide plane structure formed for a ½[1 $\bar{1}$ 0] screw dislocation intersecting two (0 1 0) free surfaces in an inclined fashion. The screw dislocation was formed with a (1 1 1) glide plane cut. The x-axis is along [0 1 0], the y-axis is along [0 0 1] and the z-axis is along [1 0 0]. The stacking fault region is shaded in pink. The colored arrows denote the Burger's vector magnitude and direction of the Shockley partials. Also shown are the [1 1 1] (b) and [1 1 $\bar{2}$] (c) 2-D projections of the position of high-energy atoms at the screw dislocation core. Note the rotation of the screw dislocation due to Lothe's forces.
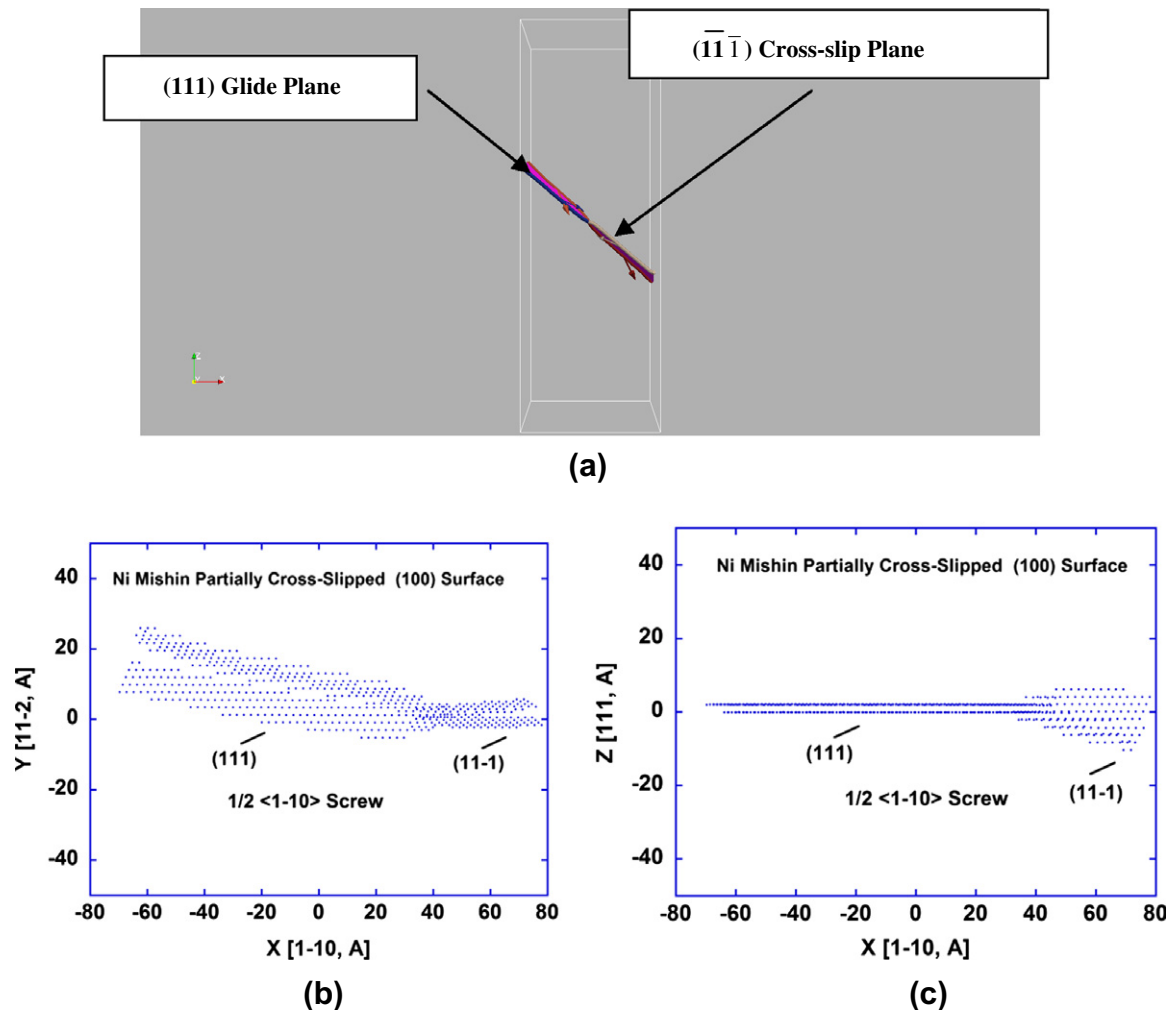
6

Fig. 5. A 3-D dislocation line representation (a) of the partially cross-slipped structure formed for a ½[1 1̄ 0] screw dislocation intersecting two (0 1 0) free surfaces in an inclined fashion. The screw dislocation was formed with a (1 1 1) glide plane cut. The *x*-axis is along [0 1 0], the *y*-axis is along [0 0 1] and the *z*-axis is along [1 0 0]. The stacking fault region is shaded in pink. The colored arrows denote the Burger's vector magnitude and direction of the Shockley partials. Also shown are the [1 1 1] (b) and [1 1 2̄] (c) 2-D projections of the position of high-energy atoms at the screw dislocation core. Note the rotation of the screw dislocation due to Lothe's forces. (For interpretation of the references to colour in this figure legend, the reader is referred to the web version of this article.)
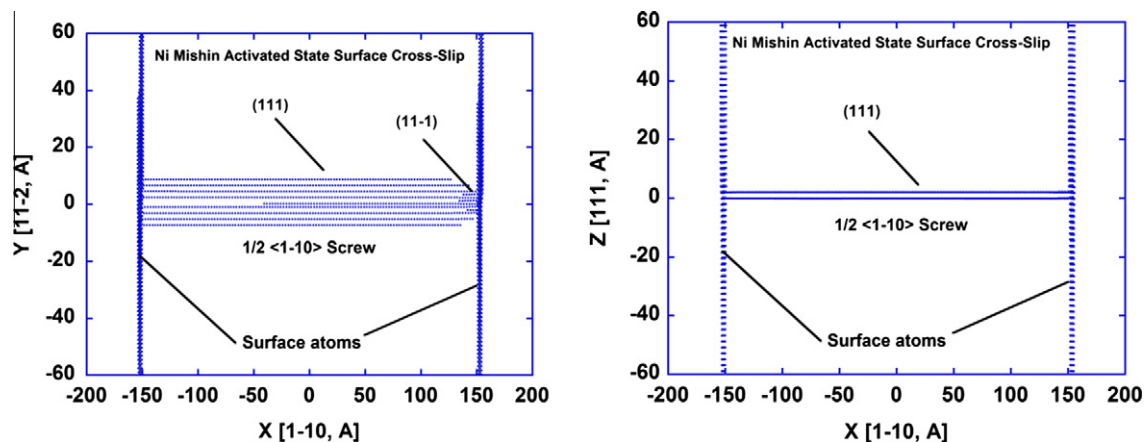

Fig. 6. The [1 1 1] (a) and [1 1 2̄] (b) 2-D projections of the position of high-energy atoms at a ½[1 1̄ 0] screw dislocation core in the activated structure. The screw dislocation was formed with a (0 0 1) cube plane cut.

tively, with these potentials. Note that these are results for the activation energy for surface cross-slip nucleation in the absence of ledge annihilation forces.

5. Discussion

The results of this work clearly show that under certain favorable conditions (favorable sense of screw dislocation, Lothe's rotation forces and minimal ledge annihilation forces) surface cross-slip can nucleate in fcc Ni and Cu. This is an important result since it qualitatively explains the profusion of cross-slip and dislocation multiplication in micron-sized fcc crystals. This finding, along with previous findings on cross-slip nucleation at screw dislocation intersections in fcc materials, should allow higher-level mesoscale models of dislocation behavior to better represent the cross-slip process without resorting to ad hoc assumptions about obstacles.

The activation energy for surface cross-slip nucleation in the absence of ledge annihilation forces has been determined to be extremely low, 0.05 eV in fcc Ni (Mishin potential) and 0.09 eV in fcc Cu, significantly lower (by a factor of 20–30) than cross-slip nucleation in isolation in bulk via the Escaig mechanism [2,4–7]. Also, the surface cross-slip nucleation energy is significantly lower than activation energy for cross-slip nucleation at mildly attractive screw dislocation intersections in fcc Ni and Cu [5–7]. However, cross-slip nucleation at mildly repulsive screw dislocation intersections has been found to be athermal with zero cross-slip activation energy [8]. The present surface cross-slip nucleation results are expected to be useful in understanding the mechanical behavior of micron-sized pillars under pure tension and compression [19,20]. However, it is unclear what effect the presence of an oxide film at the surface has on the cross-slip nucleation activation energy.

The low activation energy for surface cross-slip nucleation in fcc Ni and Cu, determined in this work are in agreement with X-ray topographic observations of preferential cross-slip at the surface in Al, Cu and Si [15–17,21–23] and in situ transmission electron microscopy observations of spontaneous cross-slip in Au foils [15–17,24]. The low activation energy for surface cross-slip nucleation in fcc Cu shown in the present work is also in agreement with surface observations of cross-slip of dislocations in alloys with very low stacking fault energies (Cu–12–14 at.% Al) when deformed in tension [15–17,25] and when fatigued [15–17,26] despite the wide dissociation of dislocations (~10 nm) and the low temperature of observation (300 K). In addition, easy surface cross-slip nucleation has been used to explain the observed operation of slip systems with low Schmid factors in fcc metals [15–17,27].

In this work, the surface cross-slip nucleation activation energy was determined in the absence of ledge annihilation and Lothe's rotation forces using molecular statics calculations. It is suggested that if ledge annihilation and Lothe's rotation forces are present, surface cross-slip nucleation will occur after the screw dislocation rotates and bends to annihilate ledges and decrease its line energy. However, such calculations are not amenable to molecular statics simulations. Large-scale molecular dynamics simulations at temperature may be required to interrogate surface cross-slip nucleation in the presence of these forces. For some geometries, Lothe's rotation forces may be asymmetric between the glide and cross-slip planes [15–17], and in such cases, it is thought that the screw dislocation would prefer to lie on a plane where the decrease in line energy due to Lothe's rotation forces is the highest.

6. Summary

The simulations in this work show the nucleation of cross-slip at a free surface in fcc Ni and Cu. The results can be summarized as follows:

(1) Two different cores structures, one fully on the glide plane and the second partially cross-slipped with the formation of a negative constriction, are found for a screw dislocation intersecting free surfaces at right angles and formed using a (1 1 1) glide plane cut. The screw dislocation is bent inwards at both free surfaces to decrease its ledge energy in the fully glide plane structure.

(2) Four different core structures—one fully on the glide plane, one fully on the cross-slip plane and the last two crystallographically equivalent, partially cross-slipped structures forming a negative constriction—are found for a screw dislocation intersecting free surfaces at right angles and formed using a (0 0 1) cube plane cut.

(3) Two different core structures, one fully on the glide plane and the other one partially cross-slipped forming a negative constriction, are found for a ½[1 −1 0] screw dislocation intersecting two (0 1 0) free surfaces in an inclined fashion. The screw dislocation rotates to minimize its line energy. The sense of screw dislocation has to be favorable for the formation of the partially cross-slipped structure.

(4) Surface cross-slip nucleation energy has been determined to be 0.05 eV in fcc Ni and 0.09 eV in fcc Cu, in the absence of ledge annihilation forces.

References

[1] Escaig B. In: Rosenfield AR, Hahn GT, Bement AL, Jr., Jaffee RI, editors. Proceedings of the Battelle Colloquium on Dislocation Dynamics. New York: McGraw-Hill; 1968. p. 655.

[2] Rao S, Parthasarathy TA, Woodward C. Phil Mag A 1999;79:1167.

[3] Bonneville J, Escaig B. Acta Metall 1979;27:1477.

[4] Rasmussen T, Jacobsen KW, Leffers T, Pedersen DB. Phys Rev B 1997;56:2977.

[5] Rao S, Dimiduk DM, El-Awady J, Parthasarathy TA, Uchic MD, Woodward C. Philos Mag 2009;89(34):3351.

[6] Rao S, Dimiduk DM, El-Awady J, Parthasarathy TA, Uchic MD, Woodward C. Acta Mater 2010;58:5547.

[7] Rao S, Dimiduk DM, Parthasarathy TA, El-Awady J, Uchic MD, Woodward C. Acta Mater 2011;59:7135.

[8] Rao S, Dimiduk DM, El-Awady J, Parthasarathy TA, Uchic MD, Woodward C. Philos Mag; submitted for publication.

[9] Plimpton SJ. J Comp Phys 1995;117:1.

[10] Stroh AN. Phil Mag 1959;3:625.

[11] Angelo JE, Moody NR, Baskes MI. Modell Simul Mater Sci Eng 1995;3:289.

[12] Mishin Y. Acta Mater 2004;52:1451.

[13] Mishin Y, Mehl MJ, Papaconstantopoulos DA, Voter AF, Kress JD. Phys Rev B 2001;63:224106.

[14] Stukowski A, Albe K. Model Simul Mater Sci Eng 2010;18:085001.

[15] Hazzledine PM, Karnthaler HP, Wintner E. Philos Mag 1975;32:81.

[16] Hazzledine PM, Shaibani SJ. In: Gifkins RC, editor. 6th International conference on strength of metals and alloys (ICSMA), vol. 1. Oxford: Pergamon Press; 1982. p. 45.

[17] Hazzledine PM. In: Bilby BA et al., editors. Fundamentals of deformation and fracture. Cambridge: Cambridge University Press; 1985. p. 385.

[18] Henkelman G, Jonsson H. J Chem Phys 2000;113(22):9978.

[19] Uchic MD, Dimiduk DM, Florando J, Nix WD. Science 2004;305:986.

[20] Greer JR, Oliver WC, Nix WD. Acta Mater 2005;53:1821.

[21] Lohne O, Rustad O. Philos Mag 1972;25:529.

[22] Minari F, Pichaud B, Capella L. Philos Mag 1975;31:275.

[23] George A, Escaravage C, Schroter W, Champier G. Cryst Latt Defects 1973;4:29.

[24] Kuhlmann-Wilsdorf D, Maddin R, Westdorp W. Appl Phys Lett 1962;1:33.

[25] Kopenaal TJ. Acta Met 1963;11:537.

[26] Desvaux MPE. Z fur Metall 1963;3:206.

[27] Lohne O. Phys Status Solidi (a) 1974;25:709.